UNIVERSITÀ
DI TRENTO

Department of Physics

Master degree in Physics

Muchas gracias aficiòn esto es para vosotros SIUUUUMMMMMM

Graduant:
Manuel Bitto

Supervisor:
Leonardo Ricci

Co-supervisor:
Alessio Perinelli

24 October 2024

Contents

Introduction

Chapter 1

An electronic analog of the Burridge-Knopoff model

1.1 Mechanical Burridge-Knopoff model

The Burridge-Knopoff (BK) spring-block model [1] is a two-dimensional system of massive blocks interconnected by springs. Additionally, each block is connected to a single moving plate by another set of springs, and connected frictionally to a single fixed plate, as shown in Fig. 1.1.

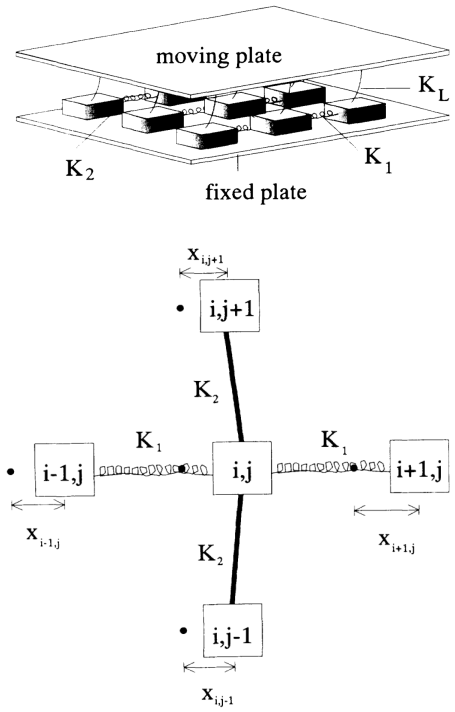

Figure 1.1: Visual representation of the Burridge-Knopoff spring-block model. K_1 and K_2 are the elastic constants, respectively, of the horizontal and vertical springs, while K_L is the elastic constant of the springs connecting the blocks and the moving plate. The figure below represents the interaction between a block and its four nearest neighbors, as a function of the displacement $x_{i,j}$. Figure adapted from Ref. [2].

The blocks are thus driven by the relative movement of the two rigid plates. When the force on one block reaches the threshold value F_{th}, the block slips, and it is reasonable to assume that the force on that block becomes zero. Then, the force on the four nearest neighbors is increased, often resulting in further slips, and an avalanche can occur.

The purpose of the BK model is the description of the dynamical behavior of real faults, whereby a constant, slow driving motion of plates produces an accumulation of "stress" up to a threshold at which such stress is released through an abrupt motion − i.e., an earthquake − of one or more of the system's constituent parts.

1.1.1 Motion of two coupled blocks

The mechanical BK model for the motion of two coupled blocks is shown schematically in Fig. 1.2.

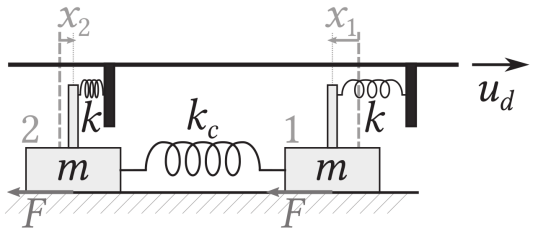

Figure 1.2: ciao

1.2 Breadboard implementation

The inductorless electronic analog of the Burridge-Knopoff model [3] is represented in Fig. 1.3. This circuit was implemented in a breadboard using 1N5817 Schottky diodes and different kinds of op-amps, namely UA741, OP07, TL081 and OP27; these op-amps were supplied with $V_{CC} = \pm 12$ V. The nominal values for the resistances and capacitors are $R = R_c = 10$ kΩ, $R_A = R_B = 10$ kΩ, $r = 1.8$ kΩ and $C = 100$ nF. The input voltages are $V_0 = 1$ V and the variable voltage V_d, while the output voltages are V and W (the subscript i is omitted).

The oscillating behavior of this circuit is shown in Fig. 1.4. The lower clamping in the Lissajous figure is intended and is due to the presence of the Schottky diodes. The frequency behavior at high voltages, namely $V_d \gtrsim 1$ V, is the same for each kind of op-amp. On the other hand, the amplitudes possess an offset which depends on the selected op-amp; nonetheless, they all exhibit a mostly linear behavior.

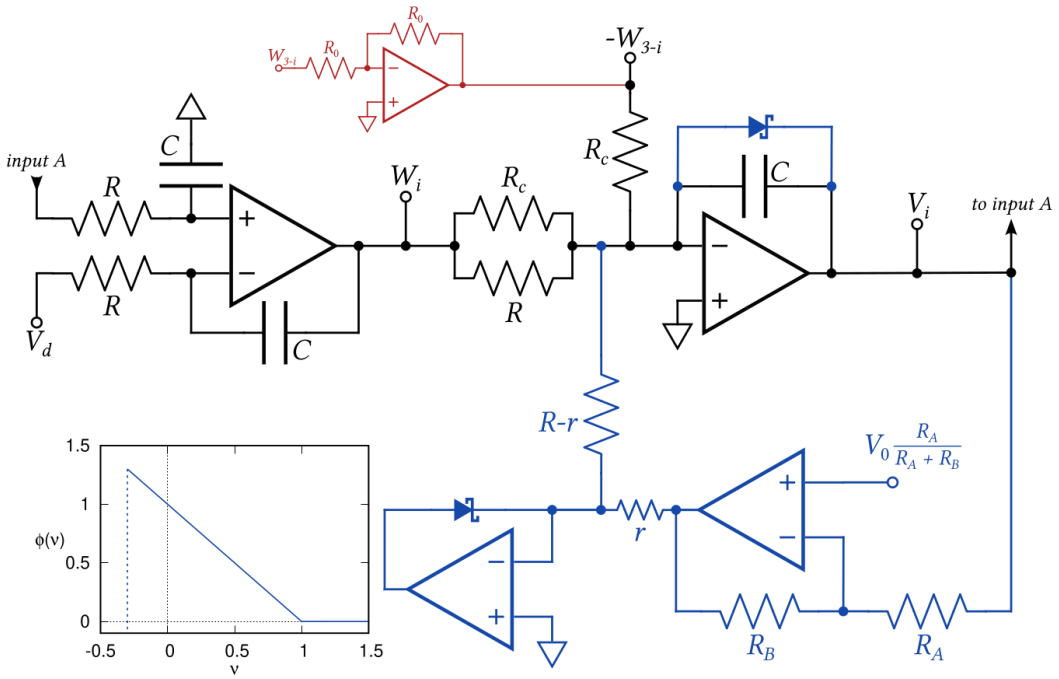

Figure 1.3: Inductorless representation of the BK model. The blue part of the network refers to the nonlinear element, whose characteristic is drawn in the bottom left plot. Figure adapted from Ref. [3].

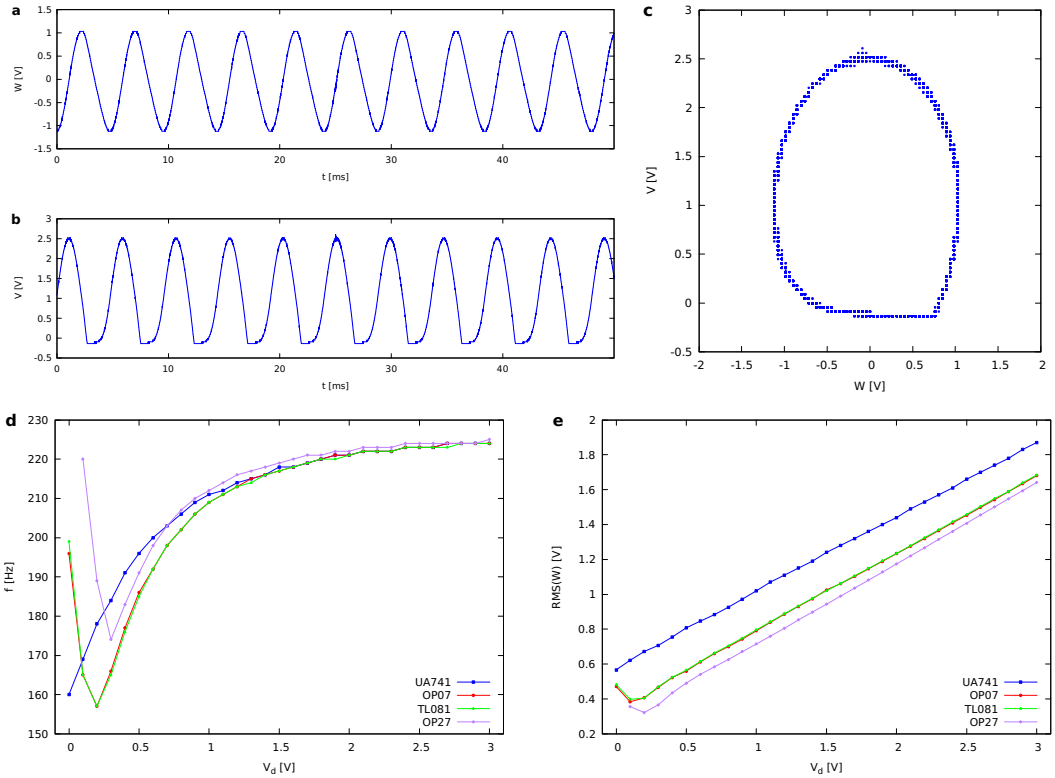

Figure 1.4: Oscillating behavior for the circuit implemented on the breadboard. (a) Plot of W and (b) of V as a function of time, for $V_d = 1$ V. (c) Phase portrait (Lissajous figure) of V versus W. (d) Frequency and (e) root mean square amplitude of the output signal W as a function of the parameter V_d and for different kinds of op-amps.

1.3 Prototypes

In order to describe the coupling between many oscillators it is not possible use the breadboard implementation of the circuit shown in Fig. 1.3, due to scalability issues. For the purpose of improving the system scalability, two smaller prototypical chips have been built. The circuit implemented in each chip is shown in Fig. 1.5. The differences between this circuit and the one used in the previous section lie in the nonlinear elements; in this case MBRA210L Schottky diodes have been used, as well as quad operational amplifiers OP470, which offer comparable performance to OP27 op-amps.

The oscillating behavior of this circuit is shown in Fig. 1.6 for both chips. These systems are much less stable with respect to the circuit implemented on the breadboard; in fact, measurements were possible only in a small range for V_d, namely $V_d \leq 1.1$ V for one chip and $V_d \leq 0.6$ V for the other one. It is also important to point out that the diode clamping is not present; in fact, it is only noticeable at voltages $V_d \lesssim 0.4$ V.

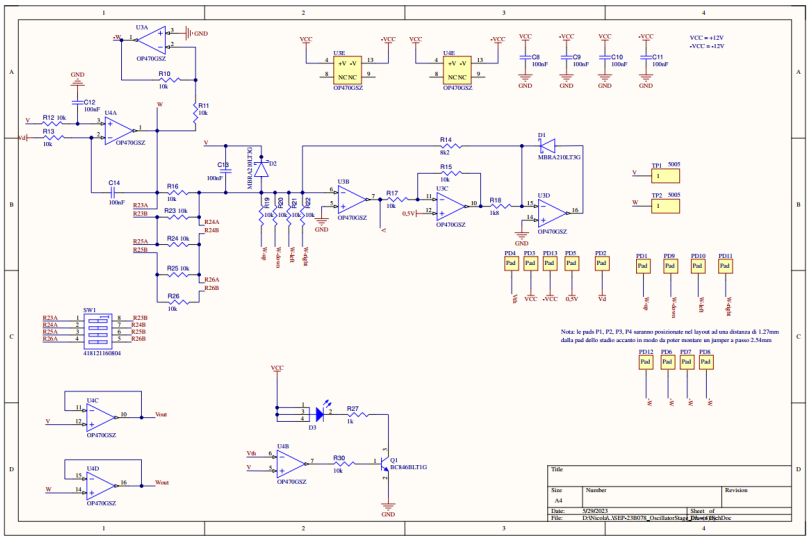

Figure 1.5: Circuit diagram of one prototypical chip.

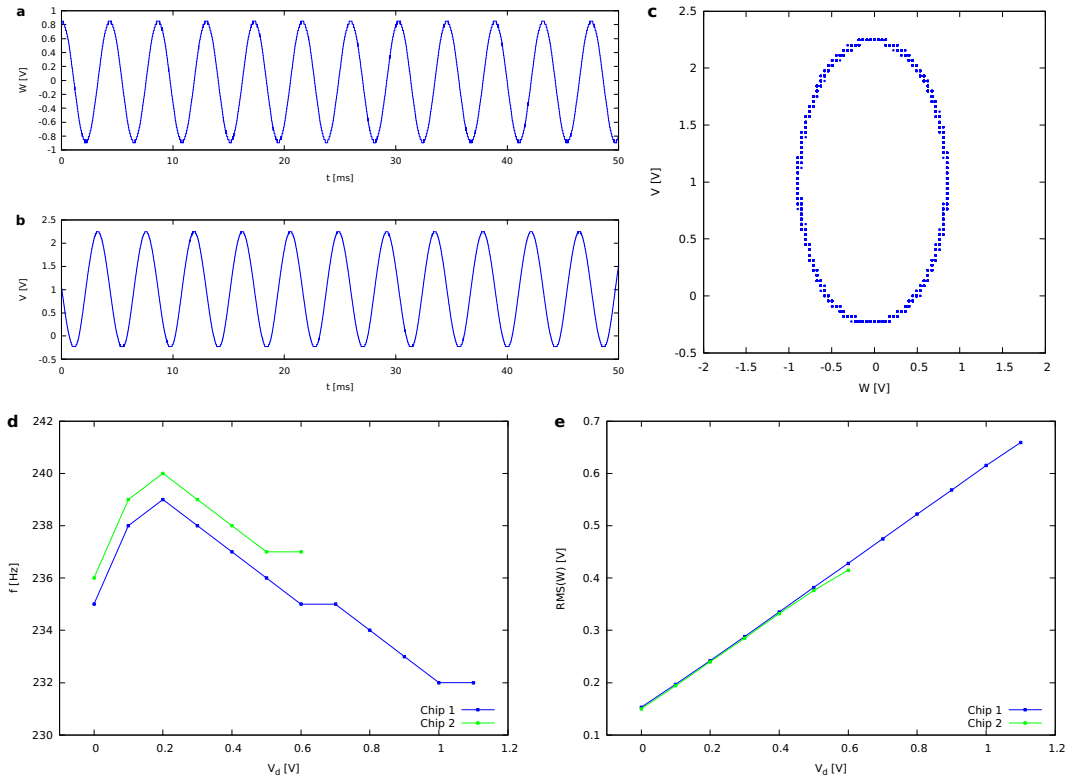

Figure 1.6: Oscillating behavior for the circuit implemented on the prototypical chips. (a) Plot of W and (b) of V as a function of time, for $V_d = 1$ V. (c) Phase portrait (Lissajous figure) of V versus W. (d) Frequency and (e) root mean square amplitude of the output signal W as a function of the parameter V_d and for the two different chips.

1.4 Board

In order to finally analyze the behavior of many coupled oscillators, a board containing 25 chips (or blocks) has been built. The circuit diagram is equivalent to the one shown in Fig. 1.5 for the prototypes, the only difference being the use of DFLS1100 Schottky diodes instead of MBRA210L ones.

The oscillating behavior is shown in Fig. 1.7. Once again, these systems are not as stable as the circuit on the breadboard; measurements were in fact taken for $V_d \leq 2.2$ V for the first two blocks. It is important to notice that in the voltage range 0.6 V $\leq V_d \leq$ 2.1 V a clamping of the output voltage V can be observed; this is not intended and is probably due to intrinsic limitations in the current.

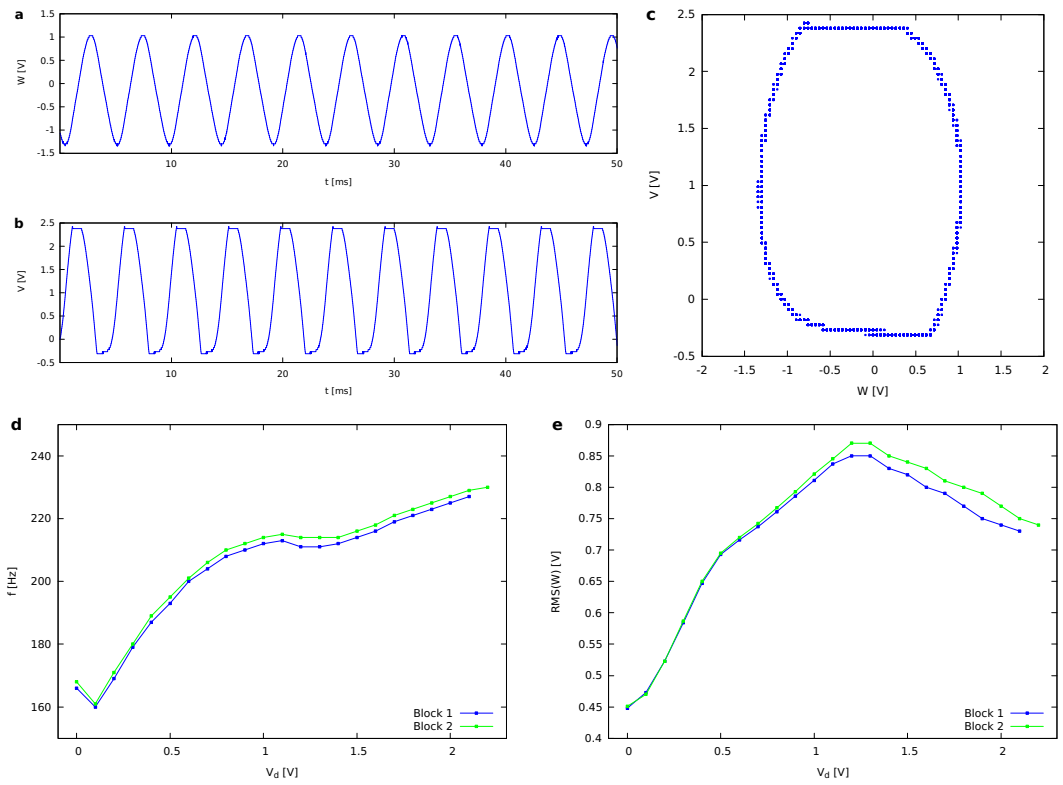

Figure 1.7: Oscillating behavior for the circuit implemented on the board. (a) Plot of W and (b) of V as a function of time, for $V_d = 1$ V. (c) Phase portrait (Lissajous figure) of V versus W. (d) Frequency and (e) root mean square amplitude of the output signal W as a function of the parameter V_d and for two different blocks.

1.5 New board

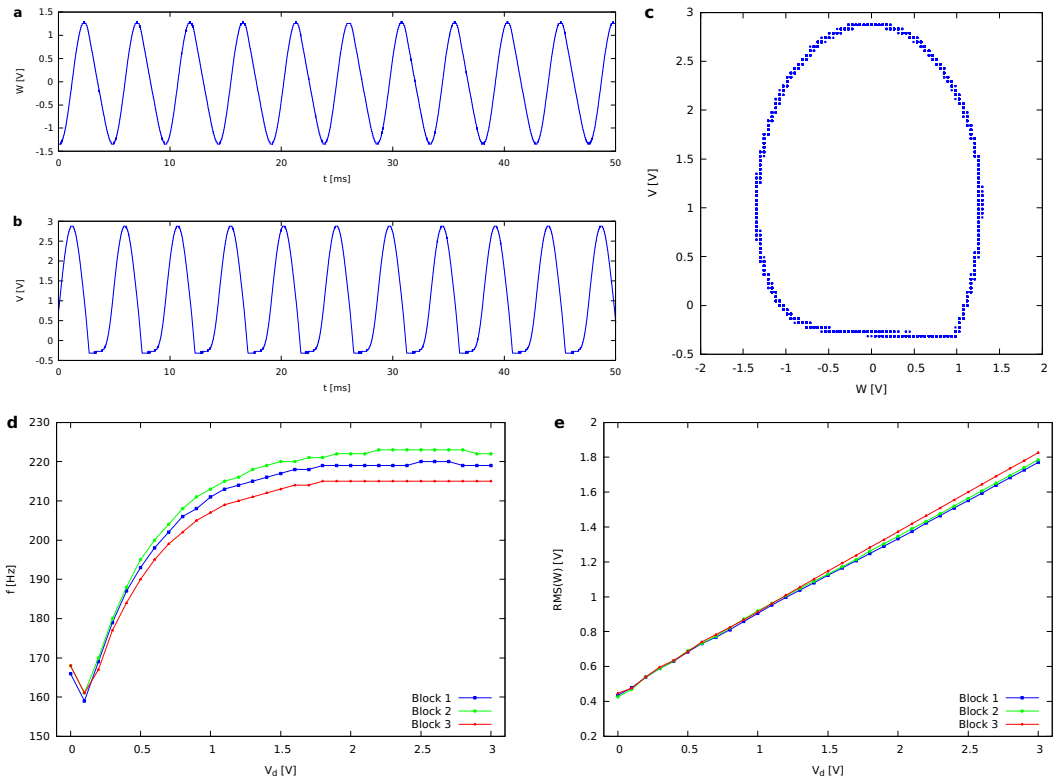

Figure 1.8: Oscillating behavior for the circuit implemented on the new board. (a) Plot of W and (b) of V as a function of time, for $V_d = 1$ V. (c) Phase portrait (Lissajous figure) of V versus W. (d) Frequency and (e) root mean square amplitude of the output signal W as a function of the parameter V_d and for three different blocks.

1.6 Conclusions

The comparison between frequency and amplitude on the three implementations is shown in Fig. 1.9. The frequency of the board is very similar to the breadboard one for voltages $V_d < 1$ V; at higher voltages there are small deviations in the board, probably due to the increased relevance of the current clamping. This might also be the reason why the amplitude behavior of the board is not linear.

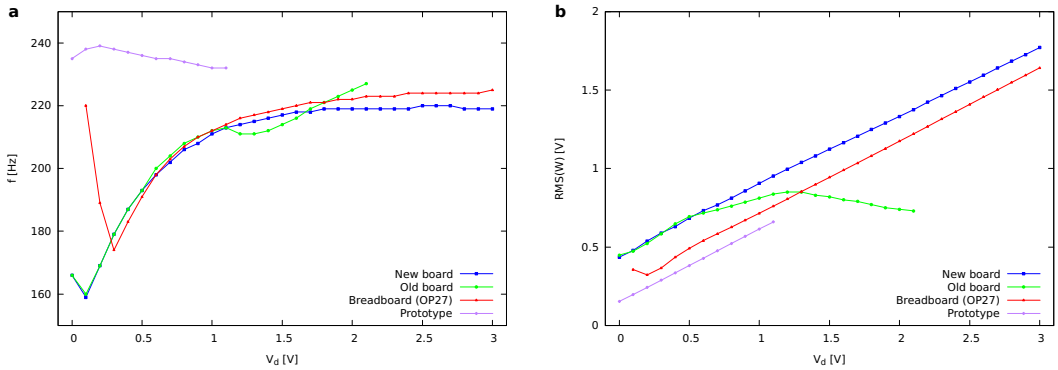

Figure 1.9: (a) Frequency and (b) root mean square amplitude of the output signal W as a function of the parameter V_d for the three implementations of the BK model, i.e. the first block of the board, the breadboard implementation with the OP27 op-amps and the first prototypical chip.

Chapter 2

Chaos analysis of multiple oscillators

2.1 Two blocks

The coupling between two oscillators is performed by connecting the inverted voltage $-W_2$ of the second oscillator to the first one and viceversa, as shown in Fig. 1.3. A chaotic behavior can be observed, as can be seen in Fig. 2.1.

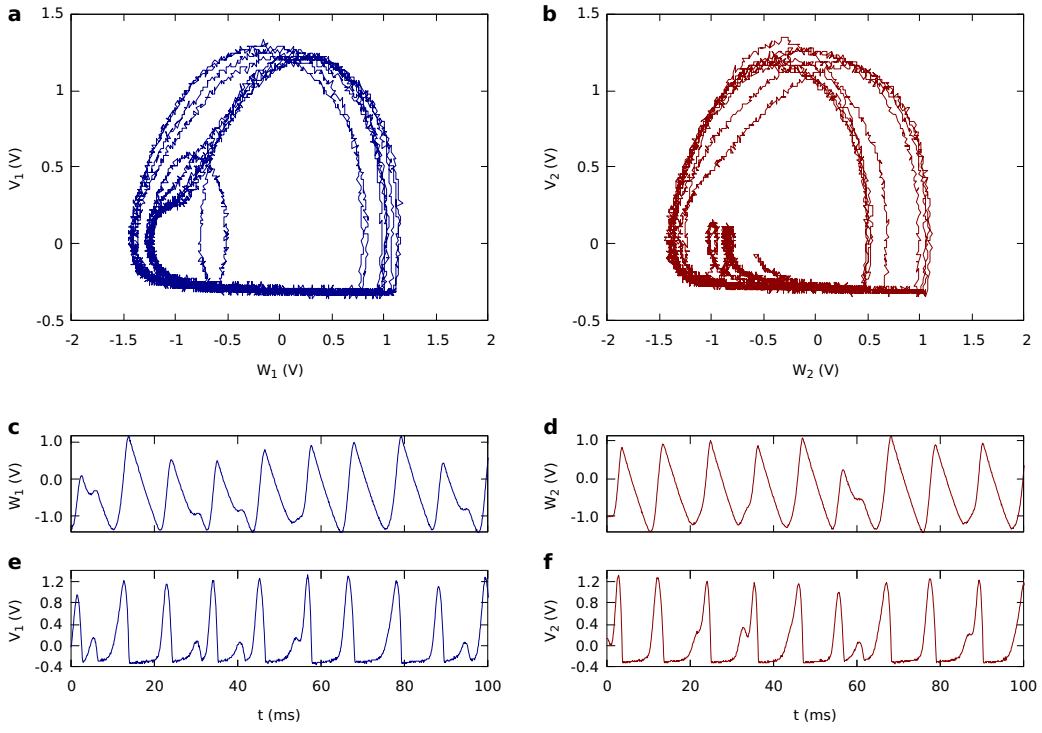

Figure 2.1: Chaotic behavior of two coupled blocks for $V_d = 0.05$ V and for a total time of 100 ms. Phase portraits of V_i vs W_i for the first (a) and second (b) block. Time series plots for W_1 (c), V_1 (e), W_2 (d) and V_2 (f).

In order to quantify the degree of chaos of this system, it is possible to carry out

an analysis

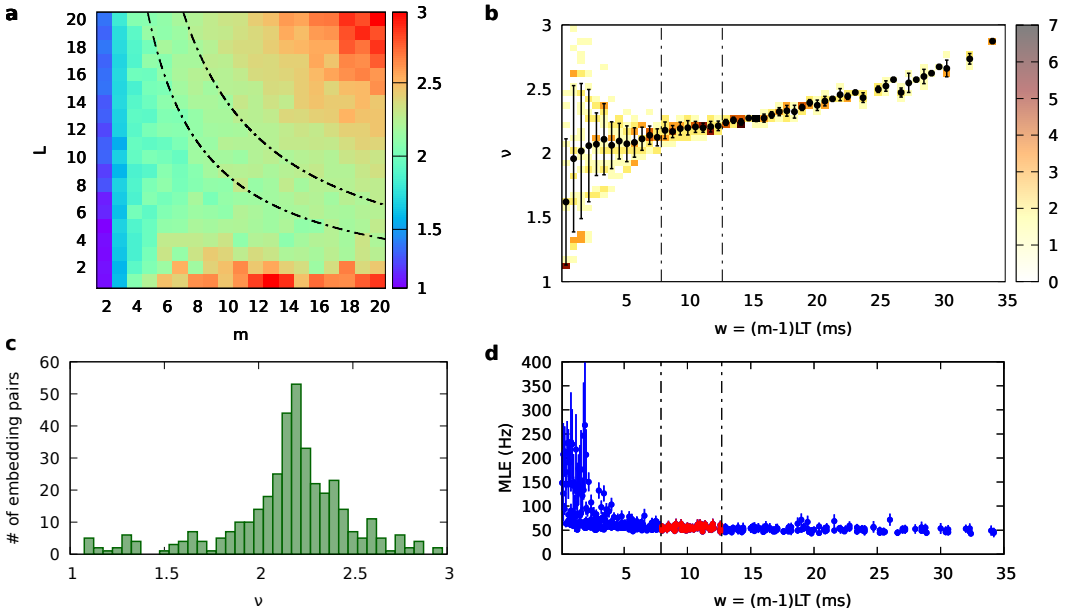

Figure 2.2: Edge

2.2 Three blocks

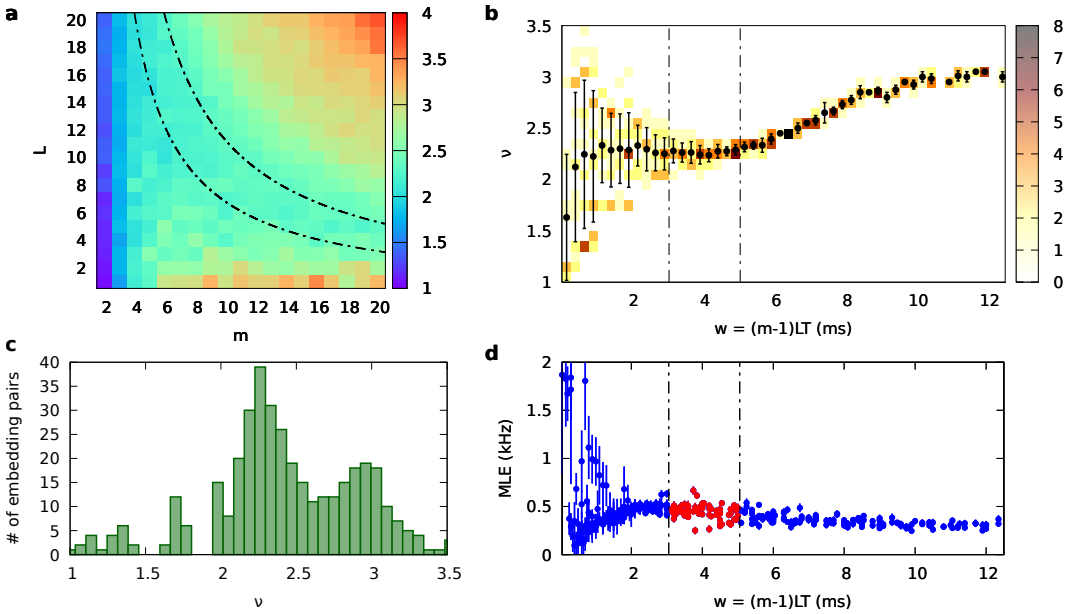

Figure 2.3: Edge

2.3 Four blocks

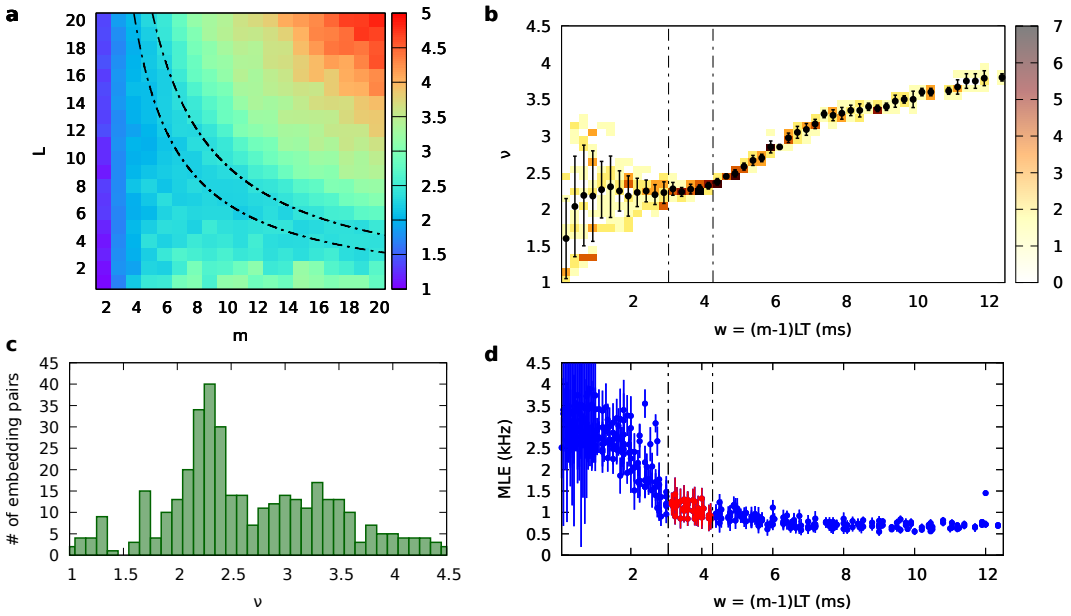

Figure 2.4: Edge

2.4 Five blocks

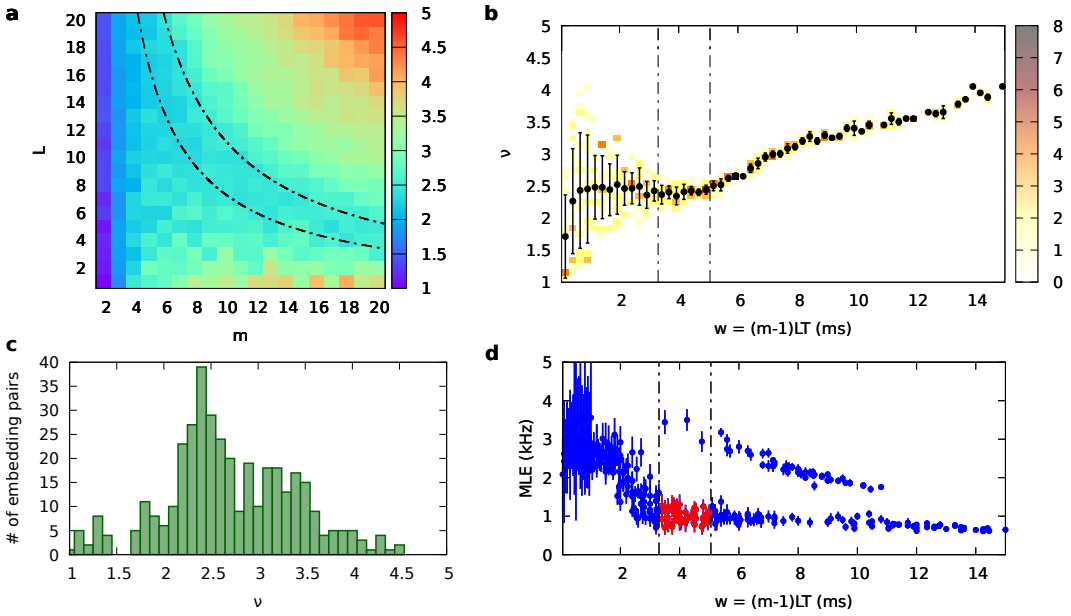

Figure 2.5: Edge

2.5 Six blocks

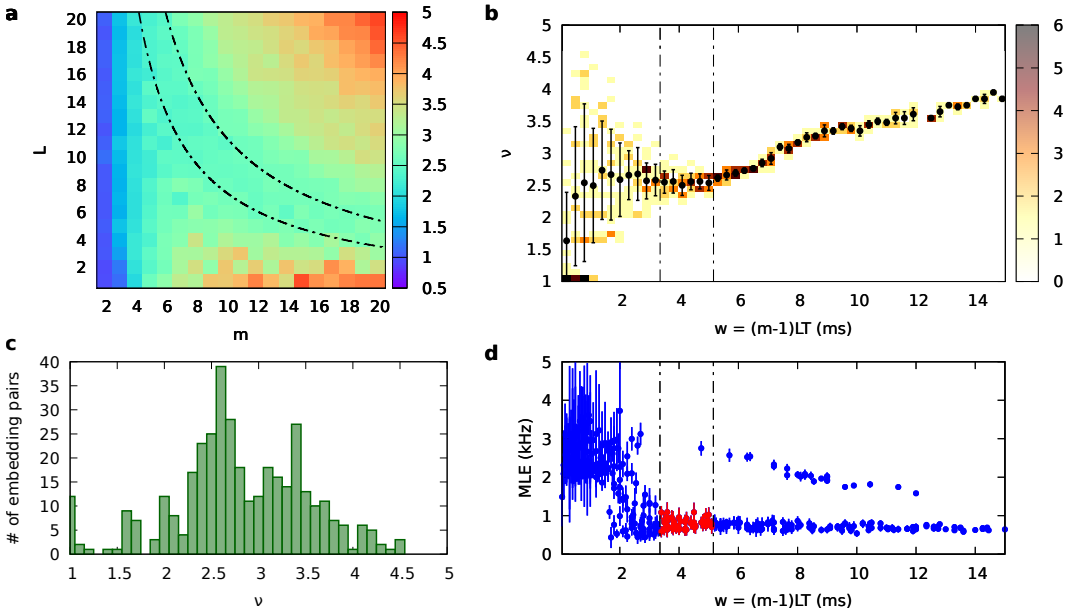

Figure 2.6: Edge

2.6 Seven blocks

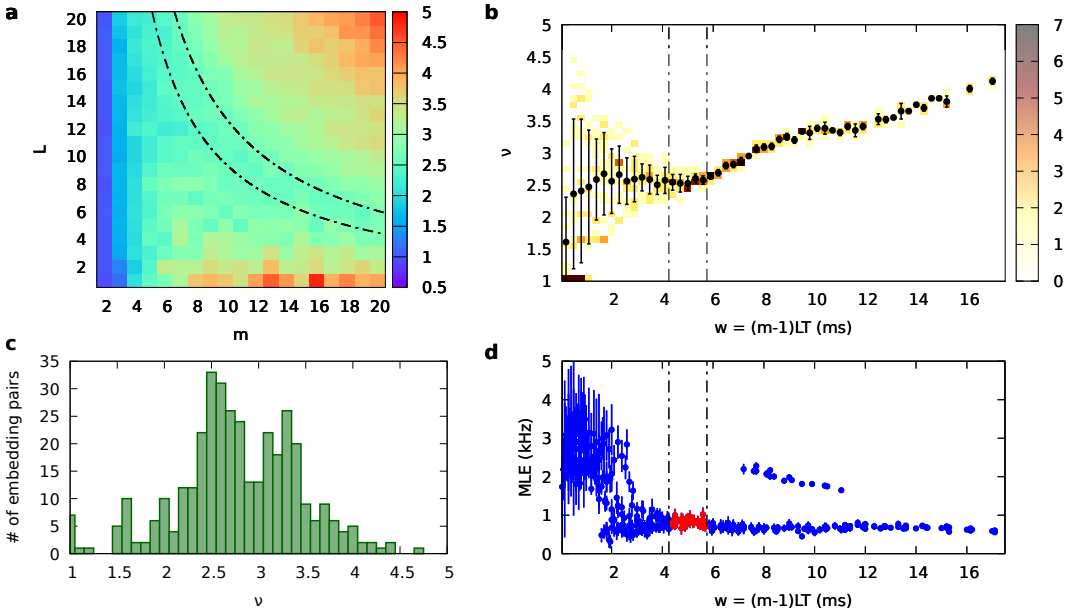

Figure 2.7: Edge

2.7 Eight blocks

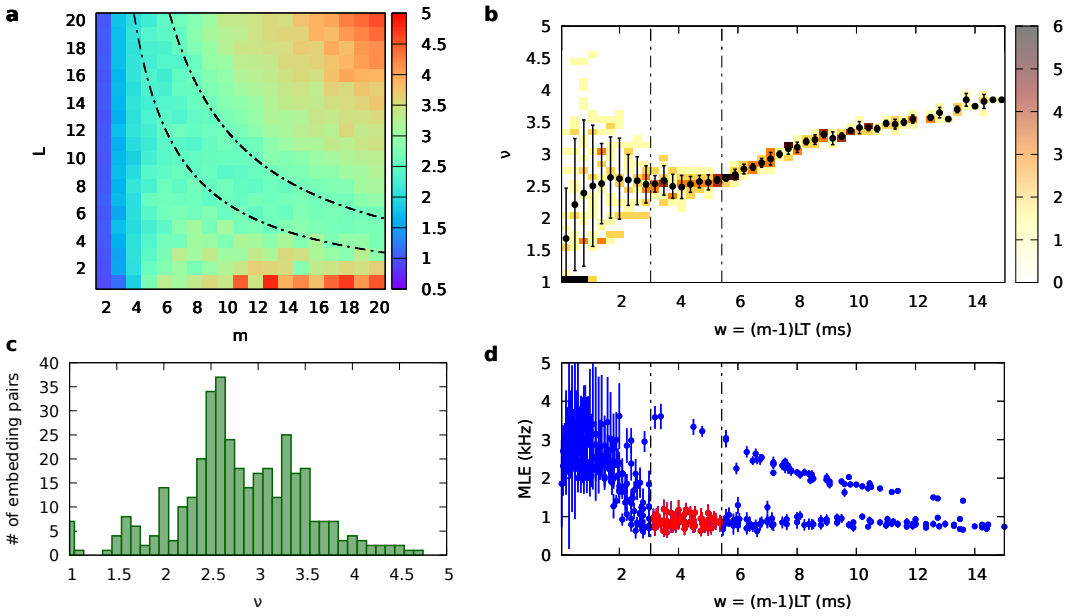

Figure 2.8: Edge

2.8 Nine blocks

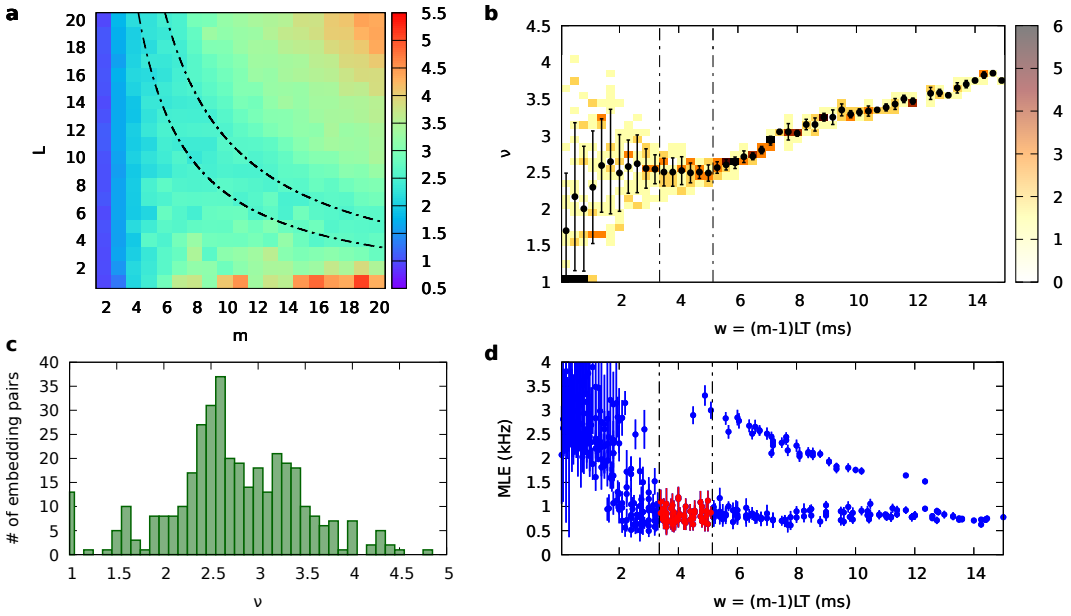

Figure 2.9: Edge

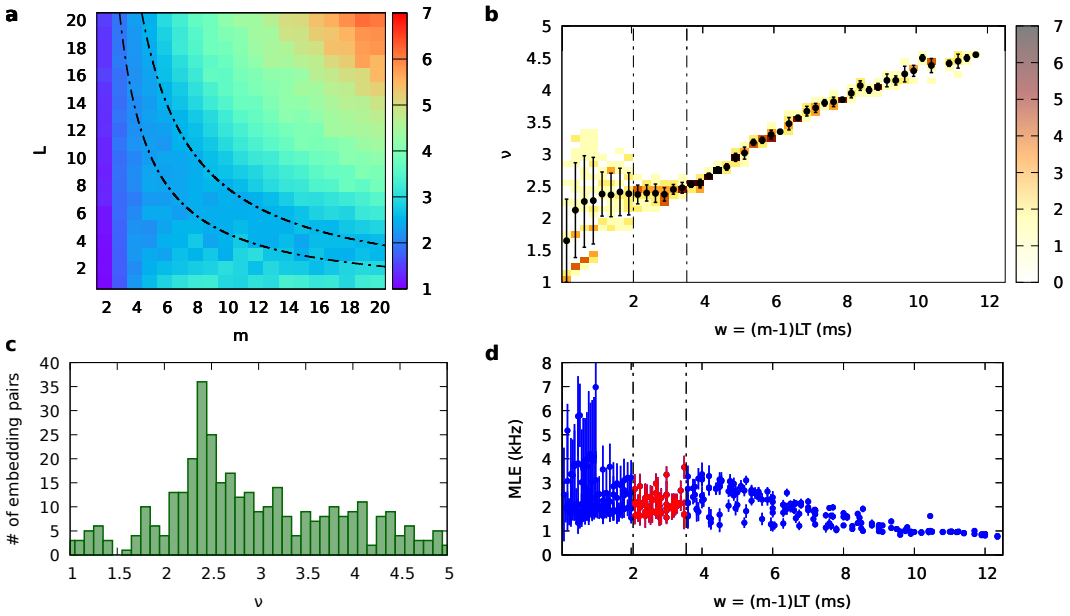

Figure 2.10: Middle

2.9 Ten blocks

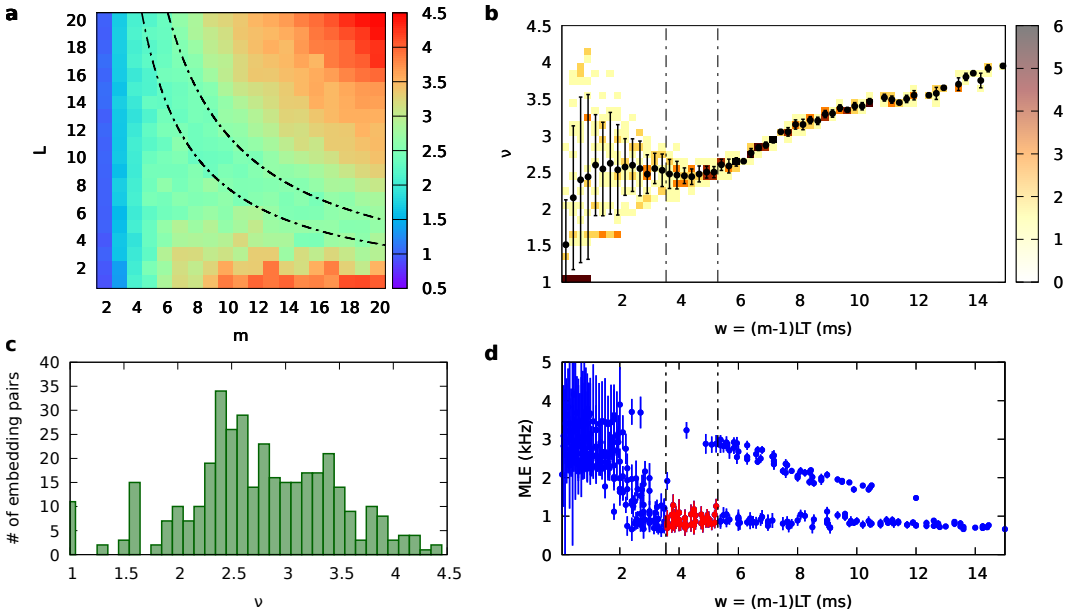

Figure 2.11: Edge

2.10 Conclusions

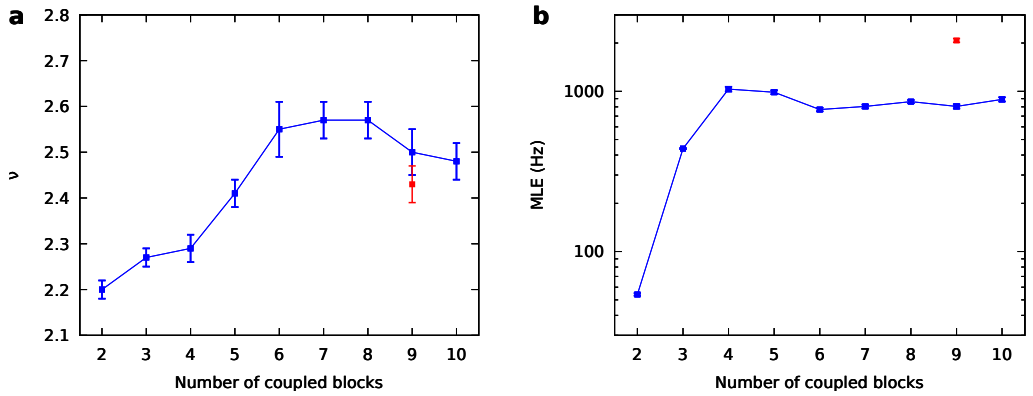

Figure 2.12: Edge (blue) and middle (red)

Chapter 3

Earthquake properties and statistical model of a fault

Bibliography

[1] R. Burridge and L. Knopoff. "Model and theoretical seismicity". In: *Bulletin of the Seismological Society of America* (1967).

[2] Zeev Olami, Hans Jacob S. Feder, and Kim Christensen. "Self-organized criticality in a continuous, nonconservative cellular automaton modeling earthquakes". In: *Phys. Rev. Lett. 68, 1244* (1992).

[3] A. Perinelli, R. Iuppa, and L. Ricci. "A scalable electronic analog of the Burridge–Knopoff model of earthquake faults". In: *Chaos 33, 093103* (2023).